Muon Propagation in Water and Ice: Overview of Various Algorithms

Wolfgang Rhode[1], Cristina Cârloganu[2]

[1] *University of California, Berkeley, USA*
Bergische Universität, Wuppertal, Germany
(rhode@wpos7.physik.uni-wuppertal.de)
[2] *Centre de Physique des Particules de Marseille, France*
(carlogan@cppm.in2p3.fr)

Abstract

Presently four large under-water and under-ice neutrino telescopes (Amanda, Antares, Baikal, and Nestor) are at different stages of operation and construction. The primary aim of these experiments is a detection of muons induced by extra-terrestrial neutrinos. The experiments will be located between 1500 mwe and 4500 mwe below the surface to shield the detectors as well as possible from the background of atmospheric muons. Therefore the knowledge of the muon flux at the location of the detector plays a role for the background suppression, the detector calibration and the signal detection. In this contribution the present knowledge on the muon propagation is discussed.

1 Introduction

The spectrum of physical problems to be addressed with large underground detectors exceeds the program which is implied by the name "Neutrino Telescopes". In principle all questions relying on particles detected deep under ground can be addressed. In the depth range of several km of water-equivalent, muons produced in the atmosphere, neutrino induced muons, and neutrino induced electrons are expected. Since the ν_μ and ν_e fluxes are comparable, but the range of a muon is larger than the length of an electromagnetic shower at the same energy, the dominant signal of neutrino induced events is for present detectors the muon flux.

The overwhelming majority of muons in all underground detectors is produced by interactions of primary nuclei (or photons) in the atmosphere either by the decay of light (π and K) or heavy (charm) mesons. The energy spectrum of the primaries can be described by a power law $\Phi = \Phi_o * E^{-\gamma_p}$. Since the dominantly produced light mesons have a comparably long lifetime they may interact instead of decaying, which steepens the corresponding muon energy spectrum by one unit ($\gamma_p + 1 \approx \gamma_{light}$) compared to that produced by the prompt decaying heavy mesons ($\gamma_p \approx \gamma_{heavy}$). Obviously the number, energy distribution and geometrical spread of the secondary muons depends on the energy and mass of the primaries and the nucleus-nucleus interaction cross sections in forward direction. Both the chemical composition and the charm production cross section are problems which are accessible in underground experiments.

However, a secondary muon undergoes typically O(1000) interactions between the surface and the underground detector. This means that in Monte Carlo calculations the systematic error per interaction will be enhanced by up to two orders of magnitude. Another error amplification occurs, if one takes additionally the muon multiplicity per interaction into account. Were the muon statistics in past generations of detectors high enough to be insignificant as error source [1], this error source would vanish completely for the present under-water or under-ice experiments. Also the systematic error due to the mountain overburden, geological structure and chemical composition of the rock becomes small in the water/ice experiments. To reduce the systematic error due to the muon propagation below the level of the uncertainties due to the first hadron interaction, air shower propagation and detector effect, one has to reduce the present uncertainty of 10^{-1} to 10^{-2} per interaction by one to two orders of magnitude.

The atmospheric muon sample is the dominant background for all investigations concerning either atmospheric or extra-terrestrial neutrino flux analyses. Depending on the depth of the experiment, the background has to be suppressed by 4 to 6 orders of magnitude for a measurement of the flux of atmospheric neutrinos, or by 6 to 8 orders of magnitude in order to detect extra-galactic neutrinos. To prove that such background rejection is possible, about this number of three dimensional muon tracks has to be generated in Monte Carlo calculations. This boundary condition sets the necessary timescale of 10^7 to 10^8 events to be generated per year.

For the primary goal of a detection of *point sources* the importance of the Monte Carlo generation of the background is smaller because the background can be obtained with x-on x-off techniques directly from the data. For transient phenomena (GRBs) the possible restriction to a time window makes the Monte Carlo generation of background even less important. In addition, the indirect consequences (such as uncertainties of the detection efficiency or energy threshold) are negligible due to the huge uncertainties in the prediction of the extra-terrestrial neutrino flux.

However, one should be aware the fact that this argument holds only for point source and GRB-search analyses. Extended sources or flux determinations (such as a measurement of the atmospheric neutrino flux to address the neutrino oscillation problem) require the full (Monte

Carlo) background calculation. Since a large number of sources may contribute to the extra-galactic neutrino flux the predicted flux for a single source is necessarily much smaller than the sum. This means that the quasi-isotropic integral flux is the strongest possible neutrino signal.

2 Muon Interactions

Apart from energy loss by *ionization*, muons may lose energy by *multiple scattering*, by *knock on* of electrons from atoms, by quantum emission in the Coulomb field of an atom (*bremsstrahlung*), by direct electron-positron *pair production*, and by the exchange of virtual photons with the atomic nucleus (*inelastic interaction*). In general these interactions cause an angular deflection Θ of the muon depending on the muon energy E, the energy transfer ν and the allowed kinematic region. The correct treatment of the kinematic region is especially important, because for the cross section calculation the integral limits in the $\Theta - \nu$ (deflection angle - energy transfer) plane may determine the results due to divergent differential cross sections at the trivial kinematic boundaries (Feynman x and y both between 0 and 1; see sect. 6). Because of the large muon mass the kinematic plane is not straightforward to determine and because of the small muon deflection the cross sections in forward direction are hard to measure. Since in underground experiments the muon loses possibly all of its energy the numerical expense for a correct Monte Carlo calculation is high: several integrals have to be calculated per interaction, neither the cross sections nor the kinematic region follow simple expressions and four possible interactions have to be tested per step.

In order to simplify the numerical procedure in Monte Carlo calculations, (1) parametrizations of the cross sections and (2) tabulated results are used. In order to speed up the calculation process, (3) the step width of the muons within the material is kept large, which also increases possible deviations. Finally, in order to keep the programs as general as possible (4) the nuclear properties of the propagation media are parametrized. All these effects sum up to an uncertainty of 10^{-1} to 10^{-2} per muon interaction. This uncertainty is sufficiently small for typical accelerator experiments, in which the muon has only several meters of absorbing material to cross and where the muon energy is determined by the curvature of the track in a magnetic field. The compilation of approximated muon cross sections, which is with small changes presently in use in most of the Monte Carlo programs [2] contains in special phase space regions deviations up to 40 % from the correct calculation.

In underground experiments the dependence of the muon intensity on the zenith angle, the chemical composition of the surrounding material and the depth profile has been measured. However, the comparison of different experiments and of experiment and analytical calculated flux prediction is aggravated for the following reasons:
In a standard analysis one first tries to correct for the fact that the muon intensity increases with the zenith angle according to a $1/cos(\theta)$ dependence, so that a depth intensity relation for 'vertical' muons is shown.[1] But this correction is wrong for the (possible) contribution of muons from the decay of heavy mesons and for the contribution of muons induced by atmospheric neutrinos. Both are important at high depths and thus on high energies and do not follow the same angular dependency. Because the overburden at large depths (or zenith angles) is a specific property of each experiment, that correction is experiment-specific. Therefore neither so-obtained depth intensity curves of experiments at different locations nor experiments and analytical calculation

[1]This is a good approximation for muons from the decay of light mesons and up to 60^o. At higher angles increasing corrections to this formula have to be made.

(as done in [3]) may be compared directly. Possible and necessary are comparisons with complete Monte Carlo generations of all components.
Another important relation is of course the relation between muon energy and range. With the simple approximation $dE/dX = a + b \cdot E$ one finds for the muon range $R(E) = 1/b \cdot \ln(1 + b/a \cdot E$ and for the minimal energy E_c at which a muon reaches the depth t $E_c = a/b \cdot (\exp(b \cdot t) - 1.)$. The coefficient a contains mainly the ionization contribution and b contains the contribution of the bremsstrahlung, the pair production and the inelastic interaction, which depend on the chemical composition of the surrounding material. Using these expressions one finds for a possible measurement of the spectral index γ of the muon flux that $\Delta\gamma \propto -\Delta b(chem)$. This illustrates that only a density correction as in [3] is not sufficient for a comparison of experiments or experiments and theory. Since b is also energy dependent the formulas given above have to be used carefully: even if a and b are interpreted as effective parameters the best effective range then depends on the spectral index (the weight of the points, with which a and b are determined from the dE/dx relation).
A third problem concerns the multiplicity of muons underground. The muon multiplicity and their spatial distribution depend on the primary interaction and the muon energy loss in the rock. For detectors with surfaces not much larger than the muon distances the detection efficiency for multimuon events of a given multiplicity depends on the muon propagation and the primary interaction. This indicates that in general a direct comparison of measured depth intensity relations with numerical calculations is inappropriate.

To achieve the accuracy necessary for muon tracking in the case of neutrino telescopes, both the theoretical input for the Monte Carlo programs and the simulation procedures have to be improved. In the following, the single contributions to the muon cross section are discussed and the status quo for the programming part will be briefly discussed at the end of the article.

3 Ionization

If the muon energy is larger than that of the orbital electrons ($\sim Z\alpha c$) muons lose energy by an ionization of the crossed material. They are not deflected. For energy losses below the threshold ν_{cut} above which energy losses are detectable in the detector, the continuous ionization energy loss is given by the Bethe-Bloch equation [4]:

$$-\frac{dE}{dx} = Kz^2 \frac{Z}{A\beta^2} \left[\frac{1}{2} ln \left(\frac{2m_e \beta^2 \gamma^2 \nu_{\text{upper}}}{I(Z)^2} \right) - \frac{\beta^2}{2} \left(1 + \frac{\nu_{\text{upper}}}{\nu_{\text{max}}} \right) + \frac{1}{2} \left(\frac{\nu_{\text{upper}}}{2E(1+1/\gamma)} \right)^2 - \frac{\delta}{2} \right]$$

$$\text{where} \quad \nu_{\text{max}} = \frac{2m_e(\gamma^2 - 1)}{1 + 2\gamma \frac{m_e}{\mu} + \left(\frac{m_e}{\mu} \right)^2}$$

is the maximum energy transferred to a free electron in a single collision, and $\nu_{\text{upper}} = min(\nu_{\text{cut}}, \nu_{\text{max}})$; $I(Z) = 75\text{eV}$ is the mean ionization potential of water and $K = 0.307075 MeV g^{-1} cm^2$. The density correction δ is taken into account with the parametrization of Sternheimer [5]. This reduction in the energy loss becomes important with the increasing polarization of the transversed media to higher energies, when single atoms can no longer be considered as isolated.

$$\delta = 0, \quad \text{if } X < X_0$$
$$\delta = 4.606X + C + a(X_1 - X)^m, \quad \text{if } X_0 \leq X < X_1$$
$$\delta = 4.606X + C, \quad \text{if } X \geq X_1$$

where $X = log_{10}(\beta\gamma)$ and the medium-dependent constants for water $C = -3.5017$, $a = 0.09116$, $m = 3.477$, $X_0 = 0.240$, $X_1 = 2.8004$ [6].

If the energy transfer in the muon electron scattering exceeds $\nu_{\text{cut}} >> I(Z)$, single electrons are *knocked on* and produce separate electromagnetic showers. A separate simulation of these electrons (δ rays) plays a role in the active volume of the detector because the deposited electromagnetic energy is indistinguishable from other energy losses. The distribution of secondary electrons as function of their energy ν is given by

$$\frac{d^2N}{d\nu dx} = \frac{1}{2}Kz^2\frac{Z}{A}\frac{1}{\beta^2}\frac{1}{\nu^2}\left[1 - \beta^2\frac{\nu}{\nu_{\text{max}}} + \frac{1}{2}\left(\frac{\nu}{E(1+1/\gamma)}\right)^2\right] \tag{1}$$

The ionization is the dominant source of energy loss for muons below the critical energy of $\approx$ 1TeV in water. The numerical uncertainty of the Bethe Bloch formula is about 1% in the GeV region, increasing to 3-4% at 1 TeV [4, 7].

4 Bremsstrahlung

The bremsstrahlung for high energy muons was calculated by Tsai [8], Rozental [9], and Petrukhin et al. [10]; the last reference offers also a parametrization for the differential cross section and has become the standard reference in the literature. A more recent and precise treatment is due to S.R. Kelner et al. [11], whose results are reviewed in the following.

The cross section can be expressed as

$$\sigma = \sigma_{el} + \Delta\sigma_a^{in} + \Delta\sigma_n^{in} \tag{2}$$

The "elastic" term (σ_{el}) denotes the cross section for bremsstrahlung on the Coulomb centre with corrections accounting for the alteration of the Coulomb field by the atomic electrons and nuclear charge distribution. $\Delta\sigma_{a,n}^{in}$ are the contributions of additional processes, described by the diagrams (Fig. 2) in which bremsstrahlung is accompanied by the changing of electronic and nuclear structure of the atom in the final state.

4.1 Elastic Bremsstrahlung

The differential cross section for bremsstrahlung in a Coulomb field is given as a function of the minimal momentum transfer $\delta \approx \frac{\mu^2\omega}{2E(E-\omega)}$, ω being the energy of the outgoing photon:

$$\sigma_{el}(E, v) = \frac{\alpha}{v}\left(2Z\frac{m}{\mu}r_e\right)^2\left(\frac{4}{3} - \frac{4}{3}v + v^2\right)\left[\ln\left[\frac{\mu}{\delta}\right] - \frac{1}{2} - \Delta_a^{el} - \Delta_n^{el}\right] \tag{3}$$

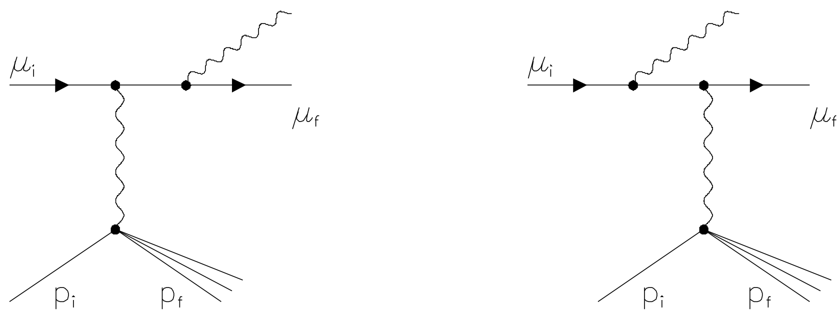

Figure 1: Feynman diagrams for bremsstrahlung on a nucleus.

The screening (Δ_a^{el}) and the nuclear (Δ_n^{el}) corrections can be parametrized as:

$$
\begin{aligned}
\Delta_a^{el}(\delta) &= \ln\left[1 + \frac{1}{\delta\sqrt{e}BZ^{-1/3}/m}\right] \\
\Delta_n^{el}(\delta) &= \ln\left[\frac{D_n}{1+\delta(D_n\sqrt{e}-2)/\mu}\right]; \qquad D_n = 1.54A^{0.27}
\end{aligned}
$$

The constant B (from the radiation logarithm[2]) is 182.7 for $Z \geq 2$ and 202.4 for hydrogen. Whereas for electrons the nuclear size correction is not significant, for muons it is large over the whole kinematic range and dominates at high v. The errors for these parametrizations are at most 1% of the muon bremsstrahlung cross section for E >100 GeV.

4.2 Inelastic Bremsstrahlung

The *excitations of the nucleus* and the deep inelastic excitations of separate nucleons (calculated in [12]) give a small (positive) correction to the cross section:

$$\Delta_n^{in} = \frac{1}{Z}\Delta_n^{el}; \ (Z \neq 1)$$

For hydrogen, the correction vanishes since the proton structure is not taken into account. For heavier elements the additional contribution of this process is of the order of 1% of the total cross section.

The conventional way of taking into account *bremsstrahlung in scattering off atomic electrons* is to replace the factor Z^2 by $Z(Z+\zeta)$ ($\zeta \approx 1$) in the bremsstrahlung cross section for scattering off a screened nucleus. However, it was shown in [13] that ζ becomes roughly constant only at high muon energies.

An important feature of muon bremsstrahlung on electrons is that the target recoil cannot be neglected. The muon cannot transfer all its kinetic energy to the photon:

$$v_{max} = \frac{m(E-\mu)}{E(E-p+m)}$$

[2]The radiation logarithm is defined as $L_{rad} = \Phi_1(\delta = 0)$, where Φ_1 is one of the two functions introduced by Bethe and Heitler to characterize the elastic scattering part in the bremsstrahlung cross section(see [8]). In the Thomas Fermi model which is usually used for the screening effect calculations, $L_{rad} = \ln\left(B\frac{\mu}{m}Z^{-1/3}\right)$. However, this model is not valid for hydrogen, which has to be calculated separately.

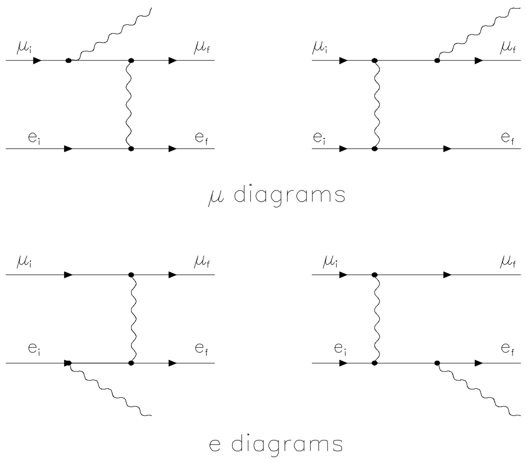

Figure 2: Feynman diagrams for bremsstrahlung on atomic electrons.

For relativistic muons, $v_{max} \approx 1/\left[1+\frac{\mu^2}{2mE}\right]$.

The two e diagrams in Fig. 2 do not exhibit the usual bremsstrahlung dependence on the photon energy $(1/\omega)$, but are proportional to $(1/\omega^2)$, similar to the elastic $\mu - e$ scattering. Therefore their contribution should be considered as a correction to the knock-on electron production, rather than to muon bremsstrahlung.

In Fig. 2 the energy of the muon can be transferred both to the photon and the electron. The energy carried away by the photons was estimated to be [13]:

$$\Delta\left|\frac{dE}{dx}\right|_{rad} = \frac{N_A Z}{A}\frac{8m\alpha r_e^2}{3}\ln\left[\frac{2E}{\mu}\right]\ln\left[\frac{2\epsilon_{max}}{m}\right]$$

whereas the total energy loss of the muons is

$$\Delta\left|\frac{dE}{dx}\right| = \frac{N_A Z}{A}m\alpha r_e^2\left(\ln\left[\frac{2E}{\mu}\right]-\frac{1}{3}\ln\left[\frac{2\epsilon_{max}}{m}\right]\right)\ln^2\left[\frac{2\epsilon_{max}}{m}\right] \quad (4)$$

with ϵ_{max} the maximum energy that can be transferred by the muon in the process, $\epsilon_{max} = \frac{2mp^2}{2mE+\mu^2+m^2}$.

The mean energy loss of a muon is associated primarily with the energy transfer to the electron. Therefore, Eq. 4 is considered as a correction to the energy loss by ionization. Additional energy losses for heavier elements amount to about 2% of the energy loss by ionization at a muon energy $E = 100$ GeV and about 4% at $E = 1$ TeV.

The contribution of the μ diagrams can be parametrized as

$$\begin{aligned}
\Delta\sigma_a^{in}(E,v) &\approx \frac{\alpha}{v}\left(2Z\frac{m}{\mu}r_e\right)^2\left(\frac{4}{3}-\frac{4}{3}v+v^2\right)\Delta_a^{in} \\
\Delta_a^{in} &\approx \frac{1}{Z}\tilde{\Phi}_a^{in}(\delta) \\
\tilde{\Phi}_a^{in}(\delta) &= \ln\left[\frac{\mu/\delta}{\delta\mu/m^2+\sqrt{e}}\right]-\ln\left[1+\frac{m}{\delta\sqrt{e}B'Z^{-2/3}}\right] \quad (5)
\end{aligned}$$

with good accuracy, compared with the numerical calculations; B'=446 for hydrogen and 1429 for materials with $Z \geq 2$.

4.3 Influence of the Medium

At very high energy and in dense materials, the multiple scattering of radiating particles imposes limitations on the energy loss of high energy particles (LPM effect). The effect describes the interference between the atomic fields of single atoms when the interaction region becomes comparable to the radiated photon wavelength and results in a suppression of the radiation cross section. The effect becomes noticeable at 10^4 TeV and leads to a 10% decrease of the bremsstrahlung energy loss at 10^6 TeV.

5 Pair production

The electron pair production (Fig. 3) is the dominant process for TeV muons; it clearly exceeds the contribution of the rest of the processes in a wide region of the energy transfers. For high energy muons, it contributes to more than 50% of the average muon energy loss.

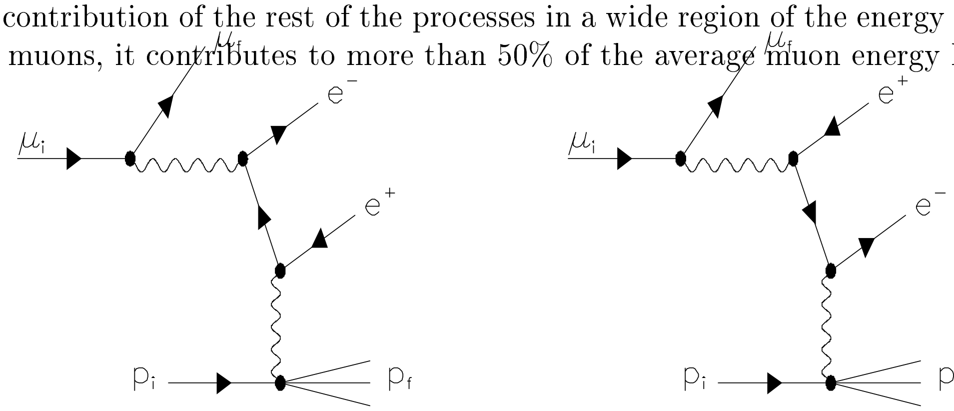

Figure 3: Feynman diagrams for pair production.

The differential cross section is usually given in terms of the muon energy (E), the energy fraction transferred to the pair ($v = (\epsilon_+ + \epsilon_-)/E$) and the asymmetry coefficient of the energy distribution of the pair ($\rho = (\epsilon_+ - \epsilon_-)/E$).

A special attention has to be paid to the screening of the nucleus by the atomic electrons, which is determined by the minimal momentum transfer to the nucleus,

$$\delta = \frac{2m^2(1+\xi)}{Ev(1-\rho^2)}, \text{ with } \xi = \left(\frac{\mu v}{2m}\right)^2 \frac{1-\rho^2}{1-v}$$

More precisely, the screening is characterized by

$$\gamma = \delta r_{at} = B\frac{\delta}{m}Z^{1/3}$$

where r_{at} is the effective radius in the Thomas-Fermi model of the atom. The constant B from the “radiation logarithm” is, obviously, the same as in the bremsstrahlung case. The screening is effective when $\gamma \leq 1$. Thus, $\gamma \ll 1$ corresponds to complete screening and $\gamma \gg 1$ implies no screening. For energies in the GeV region, the screening is negligible, beyond 10 TeV the screening region is large and has to be taken into account.

The differential cross section can be parametrized as

$$\frac{d\sigma(E,v,\rho)}{dvd\rho} = \frac{2}{3\pi}(Z\alpha r_e)^2\frac{1-v}{v}\left(\Phi_e + \frac{m^2}{\mu^2}\Phi_\mu\right) \tag{6}$$

where the e and μ indices indicate the contribution of the corresponding diagrams (Fig. 3).

The functions $\Phi_{e,\mu}$ were calculated initially in the no screening and complete screening regions [14], and were modified afterwards to allow a smooth transition between the two regions [15]. Finally, the influence of the nuclear form factors was taken into account in [16].

The results can be expressed as:

$$\begin{aligned}
\Phi_e &= \left\{[(2+\rho^2)(1+\beta)+\xi(3+\rho^2)]\ln\left(1+\frac{1}{\xi}\right)+\frac{1-\rho^2-\beta}{1+\xi}-(3+\rho^2)\right\}L_e \\
\Phi_\mu &= \left\{\left[(1+\rho^2)\left(1+\frac{3}{2}\beta\right)-\frac{1}{\xi}(1+2\beta)(1-\rho^2)\right]\ln(1+\xi)+\right. \\
&+ \left.\frac{\xi(1-\rho^2-\beta)}{1+\xi}+(1+2\beta)(1-\rho^2)\right\}L_\mu \\
L_e &= \ln\left(\frac{BZ^{-1/3}\sqrt{(1+\xi)(1+Y_e)}}{1+\frac{2m\sqrt{e}BZ^{-1/3}(1+\xi)(1+Y_e)}{Ev(1-\rho^2)}}\right)-\frac{1}{2}\ln\left[1+\left(\frac{3m}{2\mu}Z^{1/3}\right)^2(1+\xi)(1+Y_e)\right] \\
L_\mu &= \ln\left(\frac{\frac{2}{3}\frac{\mu}{m}BZ^{-2/3}}{1+\frac{2m\sqrt{e}BZ^{-1/3}(1+\xi)(1+Y_\mu)}{Ev(1-\rho^2)}}\right) \\
Y_e &= \frac{5-\rho^2+4\beta(1+\rho^2)}{2(1+3\beta)\ln(3+1/\xi)-\rho^2-2\beta(2-\rho^2)} \\
Y_\mu &= \frac{4+\rho^2+3\beta(1+\rho^2)}{(1+\rho^2)(3/2+2\beta)\ln(3+\xi)+1-\frac{3}{2}\rho^2} \\
\beta &= \frac{v^2}{2(1-v)}
\end{aligned}$$

The differential cross section given by Eq. 6 is valid for $E \geq 10$ GeV, and is non-negative for

$$\begin{aligned}
\frac{4m}{E} &= v_{min} \leq v \leq v_{max} = 1-\frac{3\sqrt{e}}{4}\frac{\mu}{E}Z^{1/3} \\
0 &\leq |\rho| \leq \rho_{max} = \sqrt{1-\frac{4m}{Ev}}\left[1-\frac{6\mu^2}{E^2(1-v)}\right]
\end{aligned}$$

The accuracy of the parametrization is on average 1% for any v and ρ in the relativistic region. Maximum deviation is 2.3%. However, the extrapolation to high muon energies has to be considered with care since the influence of the multiple scattering was not taken into account [17]. Also, for heavy elements ($Z \geq 30-40$) the Coulomb correction is important.

Due to the existence of the kinematic infrared cutoff v_{min} the differential cross section is always finite. It decreases steeply towards low energy transfers. This implies that, even if pair production contributes the most to the muon energy loss, it generates preferably rare but large energy losses.

To take into account the pair production process in collisions with electrons, in [14] Z^2 is replaced by $Z(Z+\zeta)$. The function ζ is 1 in the no screening region and it is equal to $\ln(1440Z^{-1/3})/\ln(BZ^{-1/3})$ with logarithmic accuracy in the complete screening case. This applies for the differential cross section without taking into account the nuclear form factors (as in [14] or, in [15]). The functions L_e and L_μ are then modified by the inclusion of the nuclear effects. Also the contribution of the pair production on atomic electrons is calculated separately [18]. In this reference parametrizations with an error up to 5% were obtained for the total cross section and energy loss:

$$
\begin{aligned}
-\frac{1}{E}\left(\frac{dE}{dx}\right) &= \frac{Z}{A}\left[0.073\ln\left(\frac{2E/\mu}{1+\gamma Z^{2/3}E/\mu}\right) - 0.31\right] 10^{-6}\left(\frac{\mathrm{cm}^2}{\mathrm{g}}\right) \qquad (7)\\
\sigma &= Z(\alpha r_e)^2(0.7022 l_0^2 l_z - 0.2085 l_0 l_z^2 - 0.1426 l_z^3 - 7.141 l_0 l_z + 4.259 l_z^2 \\
&+ 10.854 l_0 - 2.597 l_z - 8.174) \\
l_z &= \ln\left(\frac{2E/\mu}{1+\beta Z^{2/3}E/\mu}\right) \\
l_0 &= \ln(2E/\mu)
\end{aligned}
$$

where γ and β are constants: $\gamma = 1.95\ 10^{-5}$, $\beta = 6.4\ 10^{-4}$ for $Z \geq 2$ and $\gamma = 4.4\ 10^{-5}$, $\beta = 9\ 10^{-4}$ for hydrogen. At high energies, the cross section and energy loss for electrons approach asymptotically $1/Z$ of the corresponding values for pair production on nuclei.

An approximation for the muon transport is given by the "effective" (weighted) value for ζ

$$\zeta_{loss}^{pair}(E,Z) \sim \frac{0.073\ln\left(\frac{E/\mu}{1+\gamma_1 Z^{2/3}E/\mu}\right) - 0.26}{0.058\ln\left(\frac{E/\mu}{1+\gamma_2 Z^{1/3}E/\mu}\right) - 0.14}$$

with $\gamma_1 = 1.95\ 10^{-5}$ and $\gamma_2 = 5.3\ 10^{-5}$, respectively $\gamma_1 = 4.4\ 10^{-5}$ and $\gamma_2 = 4.8\ 10^{-5}$ for hydrogen. The accuracy is of the order of 5% for muon energies higher than 5 GeV.

6 Photonuclear Interactions

Photonuclear interactions (Fig. 4) are important for muon energies ($E \geq 10$ GeV) because the average energy loss increases linearly with the energy and at relatively high energy transfers. In the TeV region, it contributes about 10% to the muon energy loss.

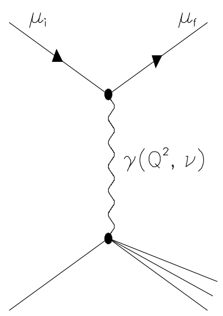

Figure 4: Feynman diagram for photonuclear interactions.

In the large Q^2 region (deep inelastic scattering) and in the low Q^2 region (photoproduction) different approaches are made. However, for the dominant processes in forward direction the main contribution to the cross section is given by the low Q^2 region ($Q^2 \ll 1$ GeV). For the scattering of a very high energy muon on a nucleus (E', $E \gg \mu$) the maximum momentum transfer to the nucleus is

$$t = Q^2_{max} = \frac{\mu^2 v^2}{1-v}$$

which is generally small.

The phenomenological generalized vector dominance (GVD) model gives a good description of the interactions of real and slightly virtual photons with hadrons. It is assumed that the photon interacts with the nucleus through vector mesons into which the photon virtually transforms. If off-diagonal terms are introduced, the model also describes large Q^2 processes, which insures a smooth overlap with the QCD predictions.

The total cross section for the photon scattering on a nucleon is a function of the photon energy ν and can be parametrized as

$$\begin{aligned}
\sigma_{\gamma N}(\nu) &= 114.3 + 1.647\ln^2[0.0213\nu]\ \mu\text{b}, \quad \text{for } \nu \in [17, 10^6\text{GeV}] \\
\sigma_{\gamma N}(\nu) &= 96.1 + \frac{82}{\sqrt{\nu}}, \quad \text{for } \nu \leq 17 \text{ GeV}
\end{aligned}$$

Since the photon nucleon cross section has been continuously measured up to a photon energy of 200 GeV and then at ≈ 20 TeV [19, 20], this approximation introduces an uncertainty of 2% below 200 GeV. Above this energy the cross section may be (within 1%) described according to [7]

$$\sigma_{\gamma N}(\nu) = 49.2 + 11.1\ln[\nu] + 151.8/\sqrt{\nu}\ \mu\text{b}$$

It was discussed that a strongly energy dependent QCD component of $\sigma_{\gamma N}$ due to a possible gluonic content of the photon might raise accordingly the muon nucleon cross section. However, the measurements of $\sigma_{\gamma N}$ (DESY experiments H1 [20] and ZEUS [19]) rule out such an increase up to a photon energy energy of 20 TeV. Theoretical considerations then limit a fast growth of the cross section even further [21].

Taking into account the nucleon shadowing, the total cross section for absorption by a nucleus becomes

$$\begin{aligned}
\sigma_{\gamma A}(\nu) &= A\sigma_{\gamma N}(\nu)\{0.75G(x) + 0.25\} \\
\text{with } G(x) &= \frac{3}{x^3}\left(\frac{x^2}{2} - 1 + e^{-x}(1+x)\right), \quad \text{for } Z \neq 1, \text{ and 1 for Z=1} \\
x &= Rn\sigma_{\rho N} \simeq 0.00282 A^{\frac{1}{3}}\sigma_{\gamma N}(\nu)
\end{aligned}$$

In the above equation, R is the nucleus radius and n the density of nucleons: $n = \frac{A}{V}$, $V = \frac{4}{3}\pi R^3$.

The parametrizations are valid up to $\nu = 10^6$ GeV, but the calculations in the region $\nu \geq 300$ GeV necessitate additional assumptions about the behaviour of the cross sections for interaction of vector mesons with nucleons.

To obtain an approximation for the differential cross section $d\sigma/d\nu$ for the inelastic scattering the double differential cross section $d^2\sigma/d\nu dQ^2$ may be integrated over Q^2.

For the case that $E_\mu >> m_\mu$ the kinematic limits are given by [1]:

$$\begin{aligned}
m_\pi + \frac{m_\pi^2}{2M} &< \nu < E - \frac{M}{2}\cdot\left(1 + \frac{m_\mu^2}{M^2}\right) \\
\frac{m_\mu^2\nu^2}{EE'} - \frac{m_\mu^4}{2EE'} &< Q^2 < 2M(\nu - m_\pi) - m_\pi^2 \qquad (8)
\end{aligned}$$

The result can be parametrized as [22]:

$$
\begin{aligned}
\frac{d\sigma}{dv} &= \frac{\alpha}{2\pi} A \sigma_{\gamma N} v \left\{ 0.75 G(x) \left[\kappa \ln\left(1 + \frac{m_1^2}{t}\right) - \frac{\kappa m_1^2}{m_1^2 + t} - \frac{2\mu^2}{t} \right] + \right. \\
&+ 0.25 \left[\kappa \ln\left(1 + \frac{m_2^2}{t}\right) - \frac{2\mu^2}{t} \right] + \\
&+ \left. \frac{\mu^2}{2t} \left[0.75 G(x) \frac{m_1^2}{m_1^2 + t} + 0.25 \frac{m_2^2}{t} \ln\left(1 + \frac{t}{m_2^2}\right) \right] \right\} \qquad (9) \\
\kappa &= 1 - \frac{2}{v} + \frac{2}{v^2} \\
m_1^2 &= 0.54 \text{ GeV}^2 \quad \text{and} \quad m_2^2 = 1.8 \text{ GeV}^2
\end{aligned}
$$

The deviation of this parametrization from the Born cross section decreases from more than 50% in the GeV region to several percent above 100 GeV. Other approximations with a comparable accuracy are discussed in [1].

7 Monte Carlo Algorithms

Independent of the calculation of the muon cross section, their translation into muon propagation codes requires a discussion. Presently various propagation codes are in use. Overviews about recent efforts to compare some of them have been given in [7, 32, 23, 24]. All of them rely basically on the parametrizations given in [2] with the corresponding uncertainties.

GEANT GEANT 3.21 [25] is a program package widely in use in High Energy Physics. Except for the photonuclear interactions the cross sections of [2] are used. The photonuclear cross section is simulated in this program by GHEISHA, leading to a mean free path which is significantly (nearly one order of magnitude) [23] larger than that of [2]. Even without this deviation the comparison of programs in [23] showed strong deviations e.g. in the residual energy after propagation through 3500 mwe standard rock, though bremsstrahlung and pair production spectra seem qualitatively to agree with those of PROPMU and FLUKA [23]. This indicates problems in the tracking algorithm. Because of these deviations an application of GEANT 3.21 to muon propagation deep underground seems not to be appropriate. Necessary would be a revision of the tracking algorithm and an update of the muon cross sections. However, in GEANT 4 which is currently being developed the error sources should be eliminated and additionally the actual cross sections should be implemented.

HEMAS The muon transport code of the Air Shower Monte Carlo HEMAS [26] is also based on the cross sections of [2]. However, in this code the energy loss (dE/dx) is first parametrized for the different cross sections and then simulated with the Monte Carlo technique. This procedure requires one more level of approximation. Accordingly the treatment of stochastical energy losses is less accurate. The comparison of the distribution of the residual energy in [23] shows a completely inaccurate description, so that it seems excluded to perform high precision calculations with this program.

MARS The program MARS [27]has not yet been systematically compared to other propagation codes. It is also based on [2], but uses instead the screening function for Bremsstrahlung by Rozental [9]. This screening function has been shown to be wrong [13] and should lead to a systematic overestimation of the total stochastic energy loss by 3.5%. An adaptation of this package to underground scenarios is not as straightforward as in the frame of other programs.

MUDEDX MUDEDX is the muon transport code of the author of [2] and also based on this reference. In its full stochastic mode it has been compared to PROPMU [28] by G. Hill [24]. Whereas the energy loss due to ionization is apparently very similar to PROPMU, the stochastic processes yield a larger mean energy loss than PROPMU. Correspondingly the muon range is shorter in MUDEDX. Differences in the average b are in the order of 5-10%. This is interesting, as in [1] the effective energy loss parameter b obtained with PROPMU was too small to allow a description of the muon flux measured with the Fréjus Detector with a spectral index of the atmospheric muon flux around 3.75 (diff).

FLUKA FLUKA [29] is, like GEANT, a complete Monte Carlo package and, using the same cross sections [2] as PROPMU, agrees perfectly with the results of this program. The drawback of the generality of FLUKA is that, for the same accuracy (cross sections), a much higher computing time is needed [23].

PROPMU The PROPMU [28] code was written for the special purposes of closed underground detectors such as MACRO, LVD or Fréjus. It performs an efficient muon propagation through large amounts of matter with the same results as FLUKA. However, due to the lack of a complete simulation of the secondary showers and their Cherenkov light it may not serve as basis for a detector Monte Carlo. Compared to the Fréjus data and the measured primary CR spectra [30] together with their interaction products in the atmosphere [31], the effective energy loss seems by some percent too small.

MUSIC Like PROPMU and MUDEDX, MUSIC [32] is a a specified muon propagation program for underground experiments. A 2% deviation in the energy loss parameter b compared to PROPMU and FLUKA can be tracked down to the use of different cross sections. Apart from this MUSIC yields results close to FLUKA and PROPMU.

Comparison with data Since the energy spectra of the primary cosmic nuclei have been measured very precisely up to an energy of 100 TeV [30] and the systematic errors due to the first interaction in the atmosphere and the development of the air shower are calculable, it seems to be appropriate to compare the three codes with measured underground data. Since the muon spectrum e.g. between 1 TeV and 6 TeV above the surface can be calculated, and the depth dependency is measured, the energy-range dependency obtained by Monte Carlo should agree within the systematic errors given by the rock overburden. For water/ice experiments this error source is obviously smaller.

If it is possible to measure not only the depth-intensity relation but also the muon energy spectrum at the location of the detector [1], even more restrictive tests of the propagation code are possible. For example in [1] the a priori error of 4% was reduced to 2.5%. Given the better systematics of water/ice, we can expect an even more significant reduction for these experiments.

8 Conclusions

With the upcoming large under-water and under-ice experiments the experimental situation has changed compared to traditional underground experiments under rock insofar as the large error sources of the mountain surface and the chemical composition of the rock become small. Though the primary goal of the detection of neutrino point sources may be reached with the Monte Carlo algorithms of present accuracy, the complete scientific potential of these experiments can only be fulfilled if the accuracy of the muon propagation can be improved by one to two orders of magnitude. Within the last ten years the theoretical understanding of the cross section calculation has been significantly improved. It is now necessary to improve existing Monte Carlo codes or invent new algorithms which allow a transfer of this improved accuracy to muon propagation.

Acknowledgement We acknowledge helpful discussions with our colleagues J.J. Aubert, A. DiCredico, G. Hill, H. Meyer, L. Moscoso, B. Price, C. Spiering, C. Wiebusch, and R. Wischnewski. WR would like to express his gratefulness for the warm hospitality he has received in Berkeley in the group of B. Price. Parts of this contribution are based on the ANTARES report [33] by CC.

References

[1] W. Rhode, Diss. Univ. Wuppertal, WUB-DIS- 93-11 (1993); W. Rhode, Nucl. Phys. B. (Proc. Suppl.) 35 (1994), 250-253; W. Rhode, this proceedings.

[2] W. Lohmann, R. Kopp, R.Voss, Energy loss of muons in the energy range 1-10000 GeV, CERN 85-03.

[3] Bugaev et al., hep-ph/9803488v2, Jun. 1998

[4] Particle Data Book. Review of Particles properties, July 1996, Phys. Rev. D 54, 132.

[5] R.M. Sternheimer, Phys Rev 88-851, 1952
R.M. Sternheimer, Phys Rev 183-511, 1956.

[6] R.M. Sternheimer, M.J. Berger, S.M. Seltzer, Atomic Data and Nuclear Data Tables 30, 261-271 (1984).

[7] R.P. Kokoulin, Nucl. Phys. B (Proc. Suppl.) 70 (1999) 475-479.

[8] Y.S. Tsai, Rev. Mod.Phys. 46 (1974) 815.

[9] Rozental, L., Sov. Phys. Usp. 11 (1986) 49

[10] A.A. Petrukhin, V.V. Shestakov, Canad. J. Phys., 46, S377, (1968).

[11] S.R. Kelner, R.P. Kokoulin, A.A. Petrukhin, About Cross Section for High Energy Muon Bremsstrahlung, Preprint of Moscow Engineering Physics Inst., Moscow, 1995, no 024-95.

[12] Yu.M. Andreyev, L.B. Bezrukov, E.V. Bugaev, Physics of Atomic Nuclei (Yad.Fiz), 57, 2066 (1944).

[13] S.R. Kelner, R.P. Kokoulin, A.A. Petrukhin, Bremsstrahlung from Muons Scattered by Atomic Electrons, Physics of Atomic Nuclei, Vol 60, No 4, 1997, 576-583.

[14] S.R. Kelner, Yu.D. Kotov, Muon energy loss to pair production, Soviet Journal of Nuclear Physics, Vol 7, No 2, 237, (1968).

[15] R.P. Kokoulin, A.A. Petrukhin, Analysis of the cross section of direct pair production by fast muons, Proc. 11th Int. Conf. on Cosmic Ray, Budapest 1969.

[16] R.P. Kokoulin, A.A. Petrukhin, Influence of the nuclear form factor on the cross section of electron pair production by high energy muons, Proc. 12th Int. Conf. on Cosmic Rays, Hobart 6 (1971), A 2436.

[17] F.F. Ternovsky, ZhETF, 37, 1010, 1959.

[18] S.R. Kelner, Pair creation on atomic electrons, Preprint of Moscow Engineering Physics Inst., Moscow, 1997, no 016-97.

[19] ZEUS Collaboration, Z. Phys. C, 63 (1994) 391.

[20] H1 Collabortation, Z. Phys. C, 69 (1995) 27.

[21] Drees, Halzen, Phys. Rev. Lett. 61(275) 1989.
Fletcher, Gaisser, Halzen, Phys. Rev. D45, 377-381, 1992, Erratum ibid D45: 3279, 1992.

[22] L.B. Bezrukov and E.V. Bugaev, Nucleon shadowing effects in photonuclear interactions, Sov. J. Nucl. Phys. 33(5), May 1981.

[23] G. Battistoni et al., NIM A 394 (1997) 136-145

[24] G. Hill, AMANDA, internal communication

[25] GEANT - Detector Program and Simulation Tool. CERN Program Library Long Writeup W5013, Geneva, October 1994.

[26] C. Forti et al., Phys. Rev. D42 (1990) 3668; H. Bilokon et al., in: Proc. of the 10th ICRC, Moscow 1987, Vol. 9, 199

[27] N. V. Mokhov, The MARS10 code system: inclusive simulation of hadronic and electromagnetic cascades and muon transport, Fermilab report FN-509 (1989)

[28] P. Lipari and T. Stanev, Phys. Rev. D, 44 (1991) 3543

[29] A. Fassò et al., Proc. of the IV Int. Conf. on Calorimetry in High Energy Physics, La Biodola, Italy (1993) 493.

[30] B. Wiebel-Sooth and. P.L. Biermann, Cosmic Rays, in Landoldt-Börnstein, Handbook of Physics, Springer Publ. Comp. 1998 (in press)

[31] D. Heck et al., CORSIKA: A Monte Carlo Code to Simulate Extensive Airshowers (1998) Report FKZA 6019

[32] P. Antonioli et al, A Three Dimensional Code for Muon Propagation Through the Rock: MUSIC (1997) Report INFN/AE-97/12.

[33] C. Cârloganu, Report ANTARES-PHYS-98-013 (1998)